THE JOURNAL OF COMPARATIVE NEUROLOGY 409:71–84 (1999)

Ultrastructural Change at Rat Cerebellothalamic Synapses Associated With Volitional Motor Adaptation

TIMOTHY DOUGLAS AUMANN[1]* **AND MALCOM KENNETH HORNE**[1,2]
[1]Department of Anatomy, Monash University, Clayton, Victoria, Australia, 3168
[2]Department of Neurology, Monash Medical Centre, Clayton, Victoria, Australia, 3168

ABSTRACT

Our ability to develop or modify motor skills is thought to involve persistent changes in the efficacy of synaptic transmission (synaptic plasticity) in the cerebellum. Previous work from our laboratory and others, examining synapses between neurons in the deep cerebellar nuclei and neurons in the thalamus revealed ultrastructural characteristics that have been implicated in the expression of synaptic plasticity at other locations in the brain. The present study sought evidence of ultrastructural plasticity at cerebellothalamic synapses associated with volitional motor adaptation. Adult rats were subject to 21 days of training, throughout which a novel load (overcome by predominantly shoulder adduction) was applied to the left forelimb while they fed (the right forelimb acted as an internal control). The behavioral paradigm was observed to produce a profound unilateral motor adaptation that was complete by day 15. Three days before the end of training, intracortical microstimulation was performed to identify the regions of primary motor cortex responsible for execution of shoulder adduction movements on the experimental (right) and control (left) sides of the brain. A retrograde neuronal tracer was injected into these cortical regions and the animals were returned to the training cage. Following training, small blocks of thalamic tissue containing retrogradely labeled cells were removed from the brains for ultrastructural analyses of presumed cerebellothalamic synapses (see Materials and Methods section). The only ultrastructural change observed to occur in association with the volitional motor adaptation was an increase in the proportion of dendritic shaft active zone with docked synaptic vesicles. J. Comp. Neurol. 409:71–84, 1999.

Indexing terms: synaptic plasticity; motor learning; cerebellum; thalamus

The ability of the nervous system to modify all types of behavior following practice or training is thought to be mediated by persistent changes in the efficacy of information transfer between neurons, a phenomenon known as synaptic plasticity. This idea emerged around the turn of the century with the discovery of the synapse and was later refined by Hebb (1949) and Konorski (1948). The cerebellum had been known for some time to be involved in the control and coordination of voluntary movement (Holmes, 1917), but it was not until much later that two theories emerged implicating the cerebellum in the ability of the nervous system to develop new and/or modify existing motor skills (Marr, 1969; Albus, 1971). In each of these theories, it was proposed that the site of plasticity assumed to underlie motor modification was at the synapses between parallel fibers and Purkinje cells in the cerebellar cortex. Subsequently, a large body of work has been devoted to understanding the role of the cerebellum in motor adaptation. It is now generally accepted that the cerebellum is necessary for the adaptation of at least two specific motor reflexes and that the associated synaptic plasticity is distributed between the cerebellar cortex and cerebellar nuclei (for review, see Raymond et al., 1996).

We previously described the ultrastructure of synapses between neurons in the rat deep cerebellar nuclei and neurons in the primary motor division of the thalamus (cerebellothalamic synapses). Among a number of distinguishing morphological characteristics were two that have been implicated in the expression of synaptic plasticity at other locations in the brain (Greenough et al., 1978; Carlin

Grant sponsor: National Health and Medical Research Council of Australia; Grant number: 980900.

*Correspondence to: Dr. T.D. Aumann, Department of Physiology and Biophysics, University of Washington School of Medicine, Seattle, WA 98195-7290. E-mail: taumann@u.washington.edu

Received 31 July 1998; Revised 13 January 1999; Accepted 14 January 1999

and Siekevitz, 1983; Dyson and Jones, 1984; Geinisman et al., 1989, 1996; Jones et al., 1991; Buchs and Muller, 1996): (1) active zones are formed simultaneously with dendritic shafts and spines, and (2) these active zones, particularly those formed with dendritic shafts, are extensively perforated (Aumann et al., 1994; Aumann and Horne, 1996). Cerebellothalamic synapses have similar ultrastructural features also in cat and monkey (Rinvik and Grofova, 1974a,b; Harding and Powell, 1977; Ilinsky, 1990; Kultas-Ilinsky and Ilinsky, 1991). It is possible, therefore, that cerebellothalamic synapses are capable of plasticity in association with volitional motor adaptation. The aim of the present study was to look for evidence of ultrastructural plasticity at cerebellothalamic synapses associated with volitional motor adaptation in rat.

MATERIALS AND METHODS

Behavioral paradigm

The behavioral paradigm was designed to induce a unilateral adaptation in forelimb motor activity. Restricting the adaptation to one limb allowed the other limb to act as an internal control. Over a 21-day period, animals compensated for a novel load applied to the left forelimb during feeding. The load was effected via magnetic attraction between a small "internal magnet" located subcutaneously in the forelimb and a large "external magnet" located adjacent to the food source.

To insert the internal magnet, adult (150 g) rats were anesthetized with a mixture of ketamine (70 mg/kg) and xylazine (6 mg/kg), and a 5-mm-long incision was made in the skin overlying the elbow joint. The skin was blunt dissected away from the underlying muscle, creating a "pocket" that extended from the incision to the forepaw. An epoxy-coated, disc-shaped, neodymium iron boron magnet (dimensions: 4.75 mm diameter 1 mm long) was placed through the incision into this pocket and the skin sutured. The animals were then allowed to recover for one week in standard laboratory cages with 24-hour free access to food and water prior to behavioral training. Despite not being fixed in any way to skin, muscle, or bone, the internal magnet was observed to remain in the same place in the limb throughout the training period.

The training cage contained a Perspex tunnel (dimensions: 50 mm wide $\times$ 50 mm high $\times$ 180 mm long) leading to an aluminum grill (nonmagnetic), behind which lay the only source of rat pellets. Water was available at a separate location in the training cage, where no load was applied to the experimental limb. Food and water were freely available to the animals 24 hours a day, and the animals were weighed daily to ensure adequate dietary intake.

A large external magnet was located outside the tunnel in a position where it would interact with the internal magnet only when the animals were in the tunnel and feeding (Fig. 1A–C). The external magnet was active at all times throughout the training period. The tunnel was designed so that it fitted snugly around the animals, preventing them from altering their body position relative to the external magnet. The forelimbs, however, were able to be used at all locations across the width of the tunnel. Thus, the magnitude of the load imposed on the left forelimb varied in strength from approximately 0.5 g on the very right side of the tunnel to approximately 20.0 g on the very left side. Despite this large variation, the animals were not seen to try and minimize the load on the limb by consistently using the experimental forelimb on the right side of the tunnel. The load acted in a direction perpendicular to both gravity and the longitudinal axis of the animals and was overcome by predominantly shoulder adduction.

Additional control and placebo animals were trained in exactly the same manner as the experimental animals. The placebo animals had a stainless-steel (nonmagnetic) disc of equal size and weight to an internal magnet inserted into the left forelimb, and the control animals were not subject to any pretraining surgical procedure.

The training period lasted 21 days. The animals remained in the training cage permanently throughout this period except for approximately 6 hours on day 18, when the microstimulation mapping of primary motor cortex and injection of neuronal tracer, described in the following section, took place.

Ultrastructural analyses

Three days before the end of the training period, all animals were removed from the training cage to identify the motor cortical (and thereby thalamic) areas responsible for execution of shoulder adduction movements (Fig. 2). Each animal was anesthetized with a mixture of ketamine (70 mg/kg) and xylazine (6 mg/kg) and placed in a stereotaxic headframe. A large hole was made in the bone overlying sensorimotor cortex contralateral to the left forelimb, and the cortex was kept moist throughout the procedure with a warm saline drip. A 0.5-MΩ epoxy-coated tungsten microelectrode (FHC Inc., Bowdoinham, ME) was used for intracortical microstimulation mapping of the primary motor cortex in a 1-mm^2 grid pattern (Fig. 2A). The stimulus used was a 30-msec train of 0.2-msec duration pulses at 333 Hz. Throughout each penetration, the minimum amount of current required to evoke a movement was determined at different depths below the cortical surface. Once the region producing left shoulder adduction at the lowest current intensity was identified, a smaller hole, centered at the same coordinates, was made in the bone overlying sensorimotor cortex contralateral to the right forelimb. This region was also microstimulated to verify that it produced right shoulder adduction at low current intensity. A retrograde neuronal tracer (10% dextran-biotin dissolved in 0.1 M phosphate buffer, pH 7.4; Molecular Probes Inc., Eugene, OR) was then pressure injected through a glass micropipette into both these cortical sites. The skin was sutured, and the animal was allowed to recover before being placed back in the training cage.

There is potential here for the damage caused in motor cortex by electrode penetrations to produce ultrastructural (degenerative) changes in the thalamus. Further, because more electrode penetrations were made in the right than in the left cortex, it might be argued that any differences between right and left thalamic ultrastructure could be due to differences in the extent of cortical damage. However, the effect in the thalamus of this cortical damage is likely to be minimal because of the short period of time (3 days) between cortical mapping and tissue collection, and be restricted to thalamocortical cell bodies and corticothalamic terminals. It would be surprising if there were any trans-synaptic effects on cerebellothalamic terminals, and there were certainly no obvious degenerative changes occurring in any of the synaptic profiles analyzed.

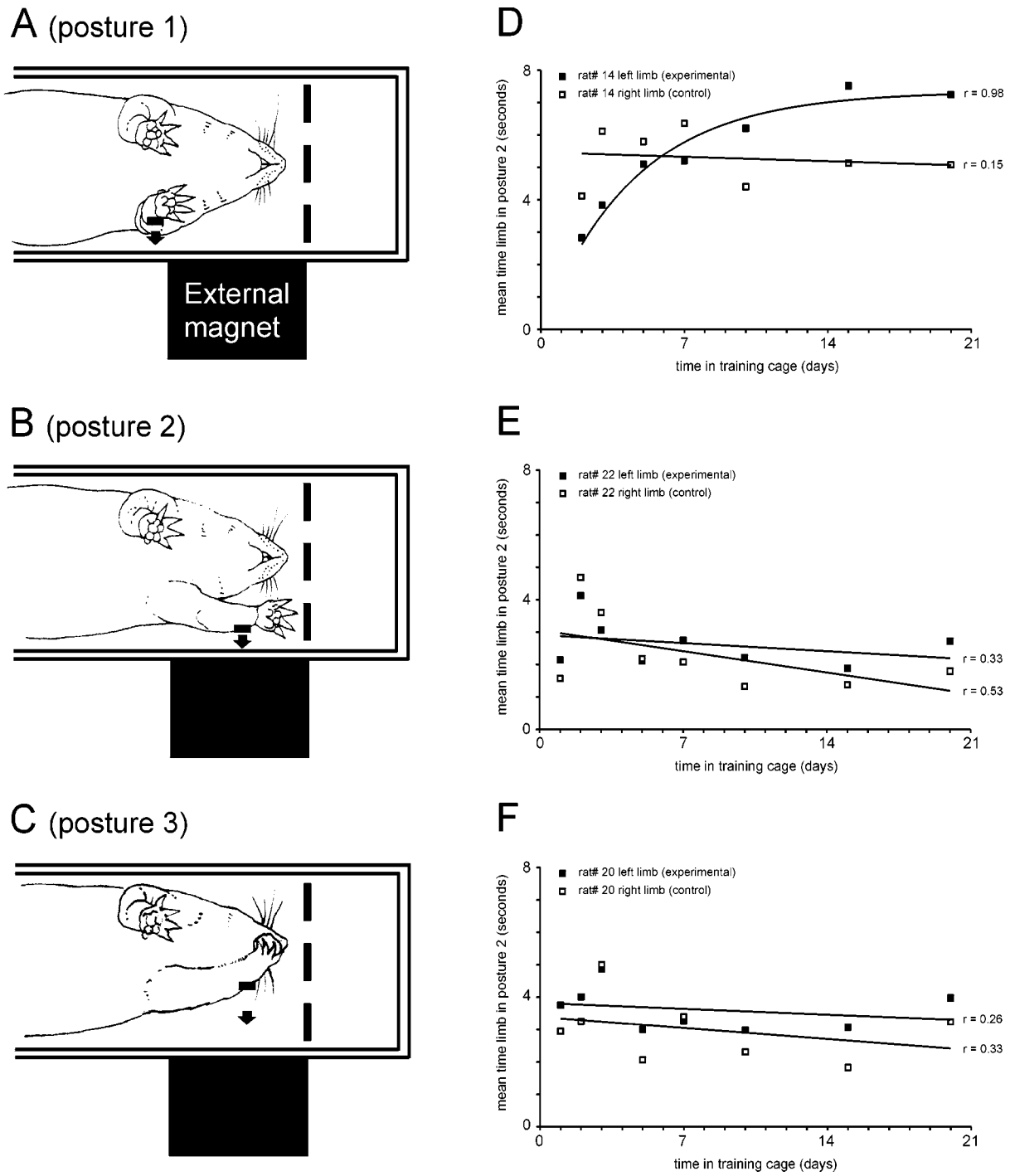

Fig. 1. **A–C:** The three predominant forelimb postures employed by the rats while feeding in the tunnel (ventral view). In each drawing, the broken vertical line represents the aluminum grill behind which lay rat pellets. The arrow shows the direction of the load imposed on the left forelimb by the attraction between the "internal" (represented as the black rectangle on the animal's forelimb) and "external" magnets. In posture 1 the forelimb was stationary on the floor of the tunnel and was used to support the weight of the animal. Posture 2 was the most active of the three postures in terms of volitional forelimb movement. Here the limb was used to reach for and manipulate pellets of food. In posture 3 the limb was used to hold small pieces of food up to the mouth. **D–F:** Plots of the mean time each limb was held in posture 2 (per single use) over the 21-day training period for an experimental (D), control (E), and placebo (F) animal. These data were obtained by measuring the cumulative time that each limb was held in posture 2 and by dividing the cumulative time by the number of uses (approximately 50 for each limb in each animal). Data from the left limb of the experimental animal have been fitted with an exponential rise to peak regression line. Data from the right limb of the experimental animal and from the left and right limbs of the control and placebo animals have been fitted with linear regression lines. Regression coefficients (r) for each line are shown.

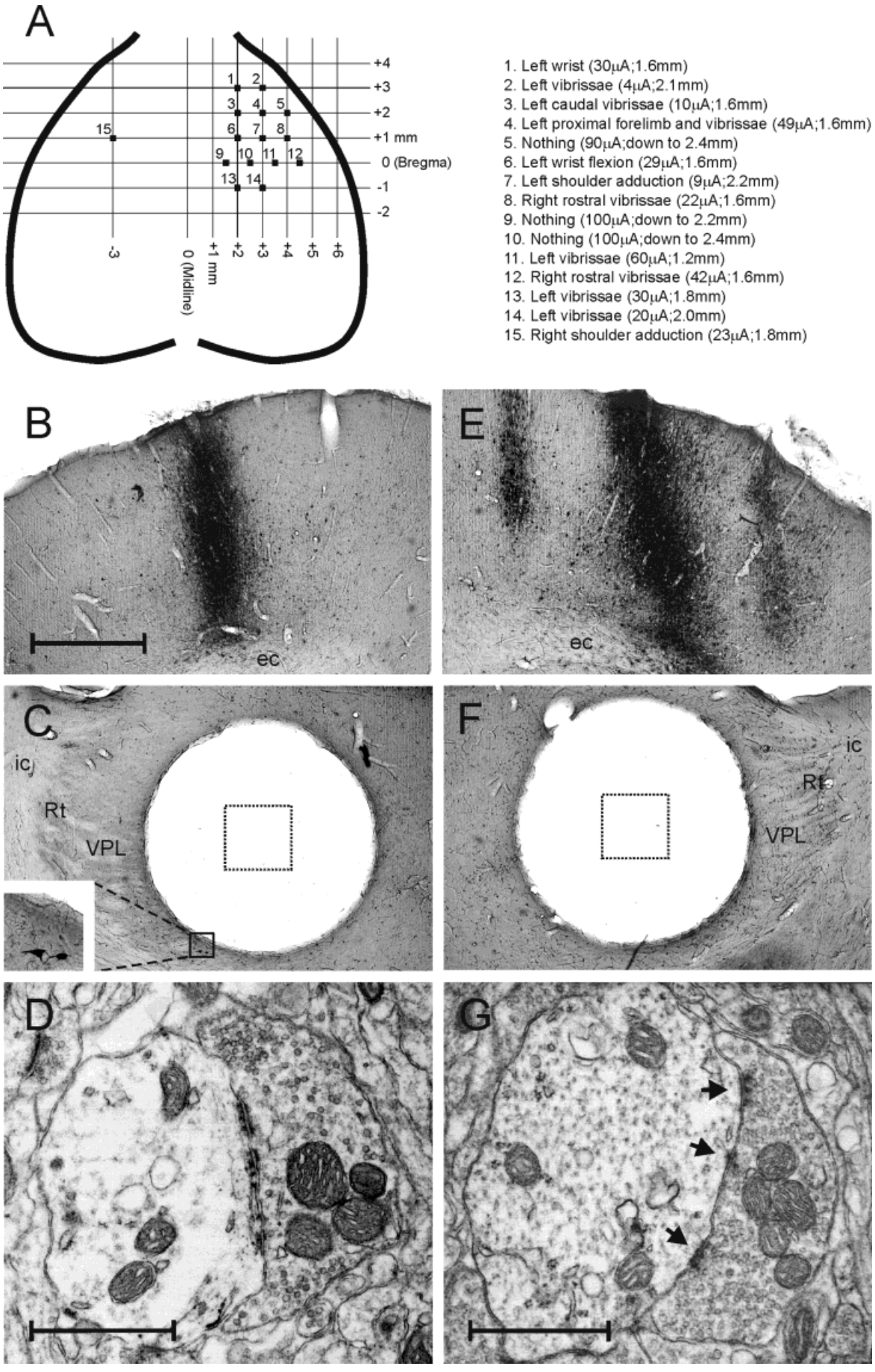
A
+4
+3
+2
+1 mm
0 (Bregma)
-1
-2
1
2
3
4
5
6
7
8
9
10
11
12
13
14
15
-3
0 (Midline)
+1 mm
+2
+3
+4
+5
+6
1. Left wrist (30μA;1.6mm)
2. Left vibrissae (4μA;2.1mm)
3. Left caudal vibrissae (10μA;1.6mm)
4. Left proximal forelimb and vibrissae (49μA;1.6mm)
5. Nothing (90μA;down to 2.4mm)
6. Left wrist flexion (29μA;1.6mm)
7. Left shoulder adduction (9μA;2.2mm)
8. Right rostral vibrissae (22μA;1.6mm)
9. Nothing (100μA;down to 2.2mm)
10. Nothing (100μA;down to 2.4mm)
11. Left vibrissae (60μA;1.2mm)
12. Right rostral vibrissae (42μA;1.6mm)
13. Left vibrissae (30μA;1.8mm)
14. Left vibrissae (20μA;2.0mm)
15. Right shoulder adduction (23μA;1.8mm)
B
ec
E
ec
C
ic
Rt
VPL
F
ic
Rt
VPL
D
G

Figure 2

At the end of the training period the animals were given an overdose of anesthetic and perfused via the aorta with 500 ml of heparinized 0.1 M phosphate buffered saline (PBS; pH 7.4) followed by 1,000 ml of 2.5% glutaraldehyde and 1% paraformaldehyde in PBS. The brains were removed and left overnight at 4°C in fixative before being serially sectioned at 100 μm in the coronal plane on a Vibratome. The sections were reacted according to the diaminobenzidine protocol detailed previously (Aumann et al., 1994) to visualize the cortical injection sites and locations of retrogradely labeled thalamic cell bodies (Fig. 2B–E). Small blocks of tissue containing these labeled cells were cut from the experimental (right thalamus) and control (left thalamus) sides of each brain (Fig. 2D–E). These blocks were postfixed in 1% osmium tetroxide, stained with 1% uranyl acetate, dehydrated in ethanol and propylene oxide, and embedded flat in Epon Araldite. One ultrathin section was cut from each block, mounted on a grid, stained with 2% aqueous uranyl acetate and lead citrate (Reynolds, 1963), and examined with a Jeol JEM100S electron microscope. All ultrathin sections were randomized and their identity concealed by a third party until data collection and analyses were complete to remove any potential bias.

Each ultrathin section was systematically scanned at 10,000× magnification and photomicrographs were taken (usually at 20,000× or 25,000× magnification) of every identified (see following) cerebellothalamic synaptic profile. In this study, cerebellothalamic synaptic profiles were identified on the basis of morphology alone. Therefore, the ultrastructural changes described in the Results section could be occurring in any one or more of the synaptic inputs to the region of thalamus examined (ventrolateral nucleus; VL). Nevertheless, we are confident that the vast majority of synaptic profiles analyzed originated from the cerebellum and, hence, that the ultrastructural changes took place in cerebellothalamic synapses. Distinguishing features of cerebellothalamic synaptic profiles include their large size, high density of round synaptic vesicles, formation of active zones simultaneously with proximal dendrites and spines, and an extensively perforated dendritic active zone that appears in profile as a series of small and distinct active "subzones" separated by gaps (Aumann et al., 1994; Sawyer et al., 1994; Aumann and Horne, 1996; for similar descriptions of cerebellothalamic synaptic profiles in cat and monkey, see also Rinvik and Grofova, 1974a,b; Harding and Powell, 1977; Ilinsky, 1990; Kultas-Ilinsky and Ilinsky, 1991). There are two other significant synaptic inputs to VL in the rat. The first and by far the most numerous of these (indeed much more numerous than cerebellothalamic synapses) have their origin in the cerebral cortex. Fortunately, these are easily distinguished from cerebellar terminals by their small size and location on distal dendrites (Aumann, unpublished observation; Kultas-Ilinsky et al., 1976; Sawyer et al., 1994; for similar descriptions of corticothalamic synaptic profiles in cat and monkey, see also Harding, 1973a,b; Grofova and Rinvik, 1974; Harding and Powell, 1977; Ilinsky, 1990; Kultas-Ilinsky and Ilinsky, 1991). The second significant input comes from the thalamic reticular nucleus and, although these synapses contact proximal dendrites, they contain pleomorphic vesicles and have a symmetric active zone (Sawyer et al., 1991, 1994; for similar descriptions of inhibitory synaptic profiles in cat and monkey, see also Harding, 1973a,b; Grofova and Rinvik, 1974; Harding and Powell, 1977; Ilinsky, 1990; Kultas-Ilinsky and Ilinsky, 1991). There are other known synaptic inputs to the rat ventral thalamus (spinal, cholinergic, noradrenergic, serotonergic, and interneuronal), but these appear to be either absent or relatively sparse in VL and/or have synaptic terminals that are much smaller than those of cerebellar origin (see, e.g., Lund and Webster, 1967a,b; Lindvall et al., 1974; Swanson and Hartman, 1975; Jones and Moore, 1977; Peschanski and Besson, 1984; Jones, 1985; Hallanger et al., 1987; Levey et al., 1987; Williams and Faull, 1987; Nothias et al., 1988; Hallanger et al., 1990).

A number of different ultrastructural synaptic parameters (see Results section) were measured from the micrographs and compared statistically across the experimental and control sides of each brain by using a Mann-Whitney rank sum test or t-test where appropriate. No corrections were made for tissue shrinkage.

All methods conformed to the Australian National Health and Medical Research Council (NH&MRC) published code of practice for the use of animals in research and were approved by the University Ethics Committee acting under the Australian NH&MRC guidelines.

Fig. 2. Summary of methods used to determine the area of motor thalamus used for data collection and analysis. **A:** Diagram of the dorsal surface of the rat cerebrum showing locations of electrode penetrations made during intracortical microstimulation mapping of the experimental (right) and control (left) sensorimotor cortices in rat 10. Figures to the right and bottom of the grid lines are stereotaxic coordinates (Paxinos and Watson, 1998). Details of the type of movement evoked at lowest current intensity for each electrode penetration (1–15) are listed to the right. **B,E:** Photomicrographs of coronal sections through the control and experimental sensorimotor cortices, respectively, of this animal. The black reaction product in B is from gliosis and bleeding caused by electrode penetration 15 and spread of the retrograde neuronal tracer injected at this site. Electrode penetrations 6, 7, and 8 can be seen in E from left to right. Retrograde tracer was injected at penetration 7. **C,F:** Photomicrographs of coronal sections through the control and experimental motor thalami, respectively, of this animal showing the areas of tissue that were removed and processed further for electron microscopy. The final ultrastructural analysis was carried out on the areas of tissue containing the highest density of retrogradely labeled cells; these areas are outlined by the dashed squares. Two retrogradely labeled cell bodies are visible in the remaining tissue in C and are shown at higher magnification in the **inset**. **D,G:** Examples of presumed cerebellothalamic synaptic profiles from the control and experimental sides, respectively, of this animal. Note the multiple dendritic active subzones within each profile and that subzones with docked vesicles (arrows) are less common on the control side. All photomicrographs in Figures 2 and 3 were scanned from the original negatives at a resolution of 300 dots per inch, and minor alterations were made in the levels of brightness, contrast, and intensity. ec, external capsule; ic, internal capsule; Rt, reticular nucleus; VPL, ventroposterolateral nucleus. B,E and C,F are at the same magnification. Scale bars = 1 mm in B, 1 μm in D,G.

RESULTS

Adaptation in motor activity induced by the behavioral paradigm

The synaptic ultrastructure data presented below was obtained from an initial group of 10 animals (six experimental, two control, and two placebo). Video recordings of their behavior were made sporadically throughout the 21-day training period. In an attempt to better quantify the alterations in motor activity induced by the behavioral paradigm, video recordings were made throughout the entire 21-day training period of a subsequent group of 12

animals (four experimental, four control, and four placebo). This was achieved by incorporating a switching mechanism that activated the video camera each time an animal entered the tunnel to feed. The behavioral data were collected from the subsequent group of 12 animals but are consistent with the less comprehensive set of data collected from the initial group of 10 animals.

During feeding the animals exhibited three distinct forelimb postures, each of which is shown in Figure 1A–C. Posture 1 was for weight bearing (Fig. 1A). Posture 2 was for manipulating food pellets (Fig. 1B). Posture 3 was for holding pieces of food up to the mouth as they were eaten (Fig. 1C). The limbs were used simultaneously in any one of the three postures or independently with each limb in a different posture. The grill was too narrow for the forepaws to pass through so the animals were restricted to manipulating pellets behind the grill with their claws only. The animals occasionally grabbed hold of the grill while in posture 2 to help stabilize the limb, but, in the main, the experimental limb was freely exposed to the full load imposed by the magnets. The teeth were also used extensively to gnaw at and break off pieces of food small enough to be brought through the grill.

Over the first two days of training, the experimental limb was dragged toward and held against the left side of the tunnel almost every time a move from posture 1 into posture 2 or 3 was attempted. Over subsequent days, the frequency of successful attempts at attaining postures 2 and 3 with the experimental limb progressively increased, as did the duration of time the limb was maintained in postures 2 and 3. By approximately day 15, the apparent use of the experimental limb was no different to the control limb, and this remained the case up to day 21. By contrast, the use of the control limb in experimental animals and both limbs in the control and placebo animals remained unchanged throughout the entire 21-day training period.

Limb usage was quantified by measuring the period of time that each individual limb was maintained in posture 2 (Fig. 1B) because this was the most active of the three postures in terms of shoulder adduction movements. Movements between the three postures was always very rapid compared with the amount of time spent in any one posture, so the period of time in posture 2 could be accurately measured as the time between movements from posture 1 (Fig. 1A) or 3 (Fig. 1C) into posture 2 and back to posture 1 or 3. The average time that each limb was maintained in posture 2 (per single usage) was plotted over the 21-day training period; representative plots for experimental, control, and placebo animals are shown in Figure 1D–F, respectively. The data confirm what we describe in the preceding paragraph. Left limb time in posture 2 progressively increased to a maximum duration in experimental animals by approximately day 15, where it remained constant to day 21 (Fig. 1D). This is in contrast to the right limb time in posture 2, which remained relatively constant over the entire 21 days (Fig. 1D). Left and right limb time in control (Fig. 1E) and placebo (Fig. 1F) animals also remained at relatively constant levels throughout the training period.

To summarize, the behavioral paradigm induced a clear unilateral adaptation in forelimb motor activity that was complete by approximately day 15 of training and remained until day 21 in experimental animals. This adaptation was not seen in the control and placebo animals. It must be emphasized that the purpose of the behavioral paradigm was to induce a change in experimental limb usage while the use of the control limb (and both limbs in the control and placebo animals) remained constant. It was not considered important for this first study that the use of one limb be more or less than the use of the other. One of the main purposes of the control and placebo animals was to control for any effect of forelimb preference on ultrastructure.

Ultrastructural change at presumed cerebellothalamic synapses associated with the motor adaptation

The data presented in this section was obtained from the initial group of 10 animals (six experimental, two control, and two placebo). Typically, five blocks of thalamic tissue were obtained from each side of the brain in each animal; from these five blocks, ultrastructural data were measured from approximately 100–200 synaptic profiles.

Measurements made from the profiles included number of presynaptic mitochondrial profiles, number of presynaptic spine profiles, presynaptic area, postsynaptic area, and spine area. These data were used primarily as an indicator of any change in size of synaptic terminals and/or their target dendrites and spines. Data relating to the active zone formed between the synaptic terminal and its target dendrite were also collected. As already mentioned, cerebello-thalamic synapses have an extensively perforated axodendritic active zone that, in profile, appears as a series of active subzones separated by gaps (Figs. 2D,G, 3A–F). Each dendritic subzone within a profile was classified as having docked synaptic vesicles (if one or more vesicles were in contact with it) or no docked synaptic vesicles (if no vesicles were in contact with it). These data were used as an indicator of the availability of the dendritic active zone to chemical neurotransmission. Measurements relating to the structure of the dendritic active zone included its total length (subzones plus gaps) and the length of each individual subzone. From these measurements, the summed length of all subzones and the summed length of all gaps were calculated. Data relating to the active zone(s) formed between the synaptic terminal and its target spine(s) were collected in the same way as for the dendritic active zone. Spine active zones were not usually perforated, but when perforations were apparent the active zones were divided into subzones and each subzone was analyzed individually. The density of synaptic profiles within the shoulder adduction region of the thalamus was not quantified in these experiments.

Data pertaining to the size of synaptic terminals, number of presynaptic mitochondria, and size of target dendrites are illustrated in Figure 4A–C; data pertaining to the axodendritic active zone are shown in Figure 5A–E; and data pertaining to the spine(s) and axospinous active zone(s) are shown in Figure 6A–E.

In summary, of all the ultrastructural parameters, the most convincing change that occurred in association with the motor adaptation was an increase in the proportion of axodendritic subzones with docked synaptic vesicles (see Figs. 2D,G, 3A–F, 5E). In four of the five experimental animals in which a comparison between the experimental and control sides of the brain was possible, the median proportion of dendritic subzones with docked vesicles was significantly ($P < 0.05$) higher on the experimental side of the brain than on the control side. In contrast, the median proportion of axodendritic subzones with docked vesicles

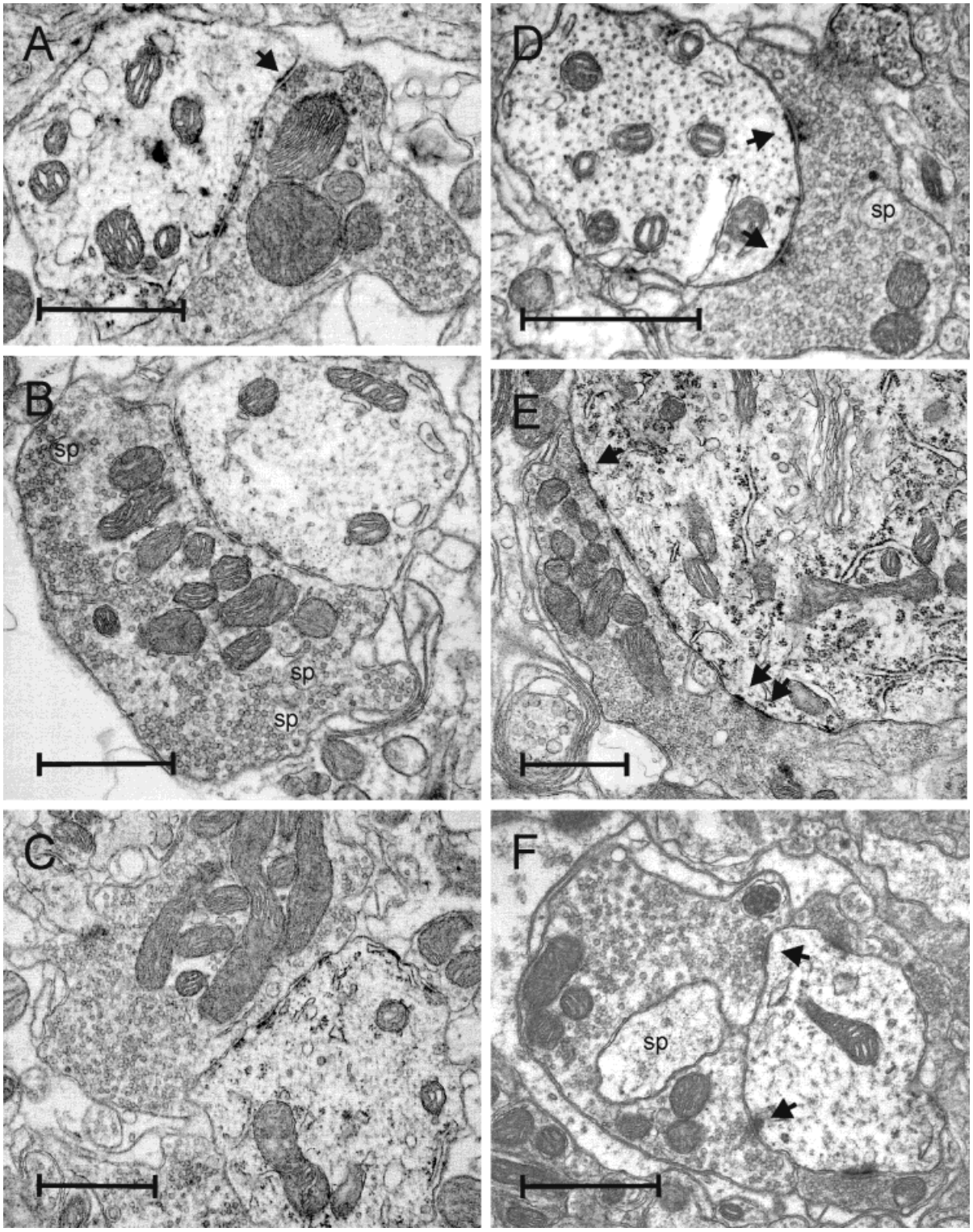

Fig. 3. Further examples of presumed cerebellothalamic synaptic profiles from the control (**A–C**) and experimental (**D–F**) sides of the brain in rat 10. Note the multiple dendritic active subzones within each profile and that subzones with docked vesicles (arrows) are less common on the control side. Although a subzone was classified as having docked vesicles if it had one or more vesicles in contact with it, nearly all subzones so classified had docked vesicles along their entire length. We are confident, therefore, that the increase in proportion of dendritic subzones with docked vesicles represents an increase in the absolute number of docked vesicles at the dendritic active zone. Spine profiles (sp) are evident in B, D, and F, but no active zones are formed with them. Scale bars = 1 μm.

was the same on either side of the brain in each of the two control and two placebo animals. Furthermore, comparing the median values across different animals, the proportion of dendritic subzones with docked vesicles was consistently ≈25% on the experimental side of the experimental animals versus ≈20% on both sides of the control and placebo animals and on the control side of the experimental animals.

There were instances of significant differences in other ultrastructural parameters, but these were limited to one or two animals in the experimental group and/or occurred also in the placebo animals. These differences included a decrease in the presynaptic cross-sectional area (Fig. 4A, rats 9 and 10), a decrease in the summed length of all dendritic subzones (Fig. 5B, rat 9), a decrease in the total number of dendritic subzones (Fig. 5D, rats 9 and 10), a decrease in the number of spine profiles (Fig. 6A, rat 10), and a decrease in the total spine cross-sectional area (Fig. 6B, rats 9 and 10). Because the number of experimental animals in which these changes occurred was relatively low, it is questionable whether they are associated with the motor adaptation. We argue that these changes are more likely due to a sampling bias, where a disproportionate number of large presynaptic profiles was included in the control datasets from these animals. Indicative of this ideal is that all these changes occurred in the same direction (decrease on the experimental side) and in the same animals (rats 9 and 10). Furthermore, these five parameters are likely to be positively correlated, i.e., the larger the presynaptic profile, the greater the number of dendritic subzones, the greater the summed length of all dendritic subzones, the greater the number of spine profiles, and the greater the total spine profile cross-sectional area (for review, see Pierce and Lewin, 1994).

If a sampling bias did occur in rats 9 and 10, it could also have implications in the data from these animals concerning the proportion of axodendritic subzones with docked vesicles (although expressing this data as proportional rather than absolute should have largely controlled for this bias). We tested this idea in these animals by comparing subsets of the data in which there was no significant difference in total number of subzones per profile (this was done systematically by removing all synaptic profiles with total number of subzones greater than eight from the experimental and control data). Whereas the difference in proportion of subzones with docked vesicles no longer achieved statistical significance in rat 9, the medians on the experimental and control sides in this animal remained 25% and 20%, respectively. By contrast, the proportion of dendritic subzones with docked vesicles did remain significantly higher on the experimental side of the brain in rat 10. Removal of this potential sampling bias, therefore, does not adversely effect the main conclusion of our study.

DISCUSSION

The present study demonstrates ultrastructural change within presumed (see Materials and Methods section) cerebellothalamic synapses associated with volitional motor adaptation in rat. Three weeks of constant exposure to an imposed load on the left forelimb during feeding induced a clear behavioral adaptation most likely involving an increase in strength of the left shoulder adduction muscles. Associated with this was an increase in the number of docked vesicles at cerebellothalamic dendritic active zones.

Before discussing the implications of the present findings, consideration must be given to their validity. A major methodological weakness of the study is that the analysis was performed on synaptic profiles rather than on whole synapses reconstructed from serial profiles. Serial reconstruction is a very time-consuming process and therefore is not a realistic option in this type of study where, because of a number of sources of data contamination, analysis of large numbers of synapses is required to detect any ultrastructural change. To detect any ultrastructural change, there is a requirement to identify those cerebellothalamic synapses involved in the execution of the movement under study. Although the regions of motor thalamus involved in shoulder adduction movements were positively identified and analyzed in these experiments, there is likely to be significant contamination of these regions with synapses involved in extraneous movements. This should not be a major problem provided large numbers of synapses are analyzed. We hasten to add, however, that analyzing large numbers of synapses will also serve to dilute any ultrastructural change that might be occurring. Indeed, we argue that this explains the unimpressive magnitude of the ultrastructural change observed (an increase from 20% to 25% in the proportion of dendritic subzones with docked vesicles). Another significant source of data contamination is the inclusion of synapses originating from the control side of the brain into the experimental data set and vice versa. This is an unavoidable consequence of the ipsilateral component of the rat cerebellothalamic projection (Aumann et al., 1994). Fortunately, the contralateral component is very much larger than the ipsilateral component so, again this is not a major problem provided large numbers of synapses are analyzed. One final potential source of contamination is by synapses arising from other areas of the brain. We are confident, however, that this is negligible because of the relative ease of identifying cerebellothalamic synapses on the basis of morphology alone (discussed in the Materials and Methods section).

Because it is unrealistic to perform the analyses on serially reconstructed whole synapses, how certain can we be that a sampling bias has not led to the observed ultrastructural changes? First, all comparisons were made between data from the experimental and control sides of the brain in individual animals. Second, the plane of section through each side of the brain (and therefore through each set of synaptic profiles) was the same. Third, there was no difference in the total number of axodendritic subzones per synaptic profile in any of the experimental, control, or placebo animals (once the sets of data from rats 9 and 10 were adjusted, as explained in the Results section). Fourth, the increase in proportion of dendritic subzones with docked vesicles on the experimental side was statistically significant in three of five experimental animals and in zero of four control and placebo animals (once the sets of data from rats 9 and 10 were adjusted). On the basis of these arguments, we believe the present findings represent a real increase in proportion of axodendritic active zone with docked synaptic vesicles.

The region of the thalamus examined in the present study transmits information from the cerebellum to the motor cortex. It was intended that the perturbation caused by the additional load on the limb would require motor

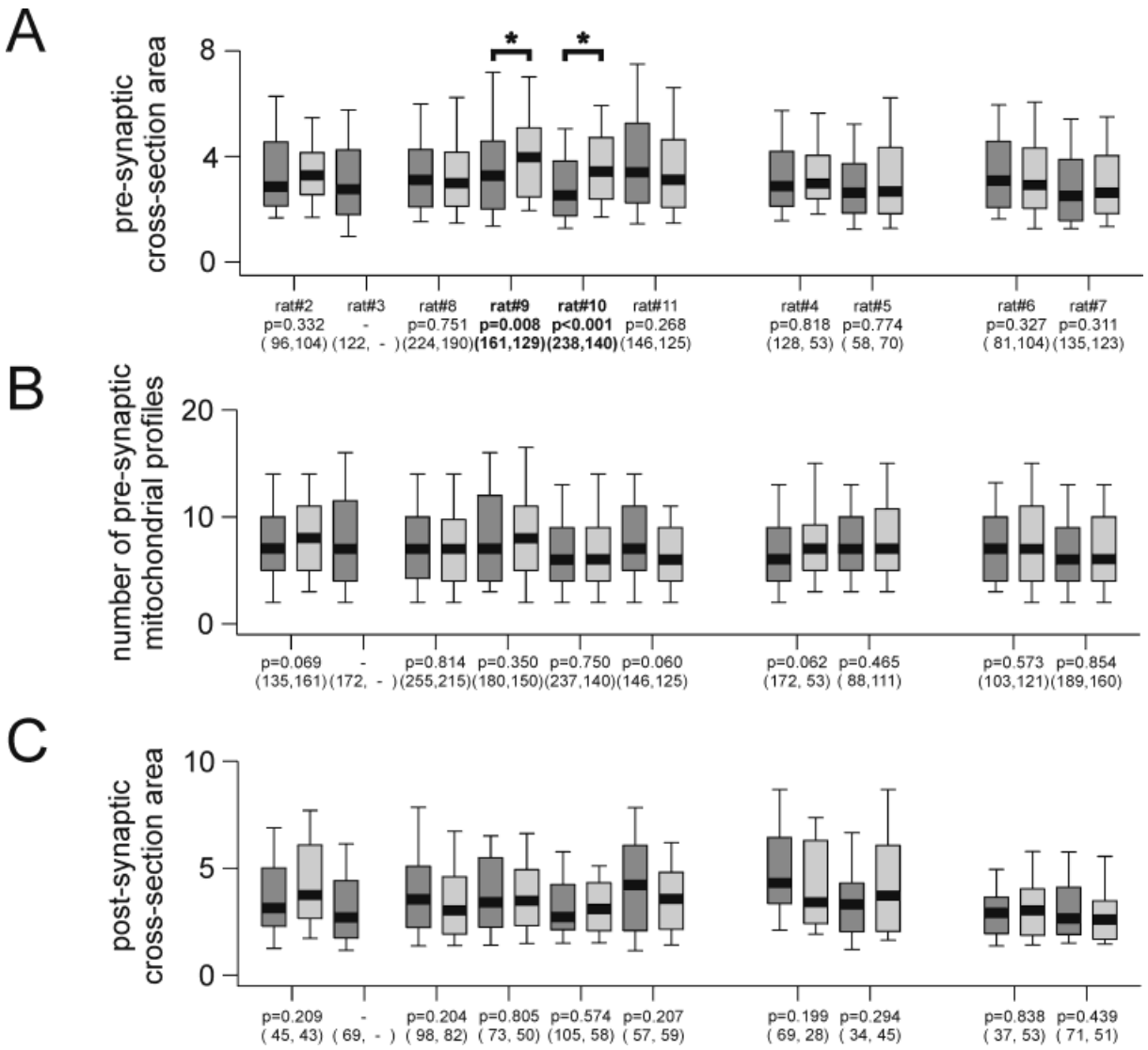

Fig. 4. Data pertaining to (**A**) the presynaptic cross-sectional area, (**B**) the number of presynaptic mitochondrial profiles per synaptic profile, and (**C**) the postsynaptic cross-sectional area. From left to right along each graph is the first group of six experimental animals (rats 2, 3, 8, 9, 10, and 11), the two control animals (rats 4 and 5), and the two placebo animals (rats 6 and 7). Each animal is represented as a pair of box-and-whisker plots (almost all the data were skewed), with the left or darker shaded plot being from the experimental side of the brain and the right plot from the control side (data from the control side of rat 3 could not be collected because of poor ultrastructure). The thick black line in each plot is the median, the upper and lower extents of the box are the 75th and 25th percentiles, respectively, and the capped bars the 90th and 10th percentiles, respectively. Below each pair of plots on the x axis are the result of the statistical comparison between the pair and the number of data points in each pair. The only significant difference found was a decrease on the experimental side in the presynaptic cross-sectional area in rats 9 and 10 (asterisks). We argue in the Results section, however, that this most likely reflects a sampling bias in these two animals rather than an effect associated with the motor adaptation.

modification that might mimic adaptation of the eyeblink and vesibulo-ocular reflexes (for review, see Raymond et al. 1996). Although much of the synaptic plasticity presumed to underlie these modifications may take place in the cerebellum, it seemed to us that if ultrastructural changes were to take place at cerebellothalamic synapses then the behavioral paradigm employed in the present study would be likely to show them. The load imposed on the forelimb was a relatively major disruption to movement and, although we were initially concerned that the animals would not be able to adapt, was clearly successful in producing motor modification. Our first objective was to demonstrate accompanying ultrastructural changes at cerebellothalamic synapses. Having achieved this objective, a more detailed examination of the task and the time course of the accompanying ultrastructural changes is planned.

We believe these findings represent an anatomical correlate of synaptic plasticity at the cerebellothalamic relay, and, because no consistent differences were found in any other synaptic parameters measured, it appears that this plasticity is largely achieved via a modification in the synaptic vesicle cycle. Some years ago, synaptic plasticity was demonstrated to underlie primitive forms of behavioral learning in the marine snail (*Aplysia californica*).

The behaviors studied were habituation and sensitization of gill and siphon withdrawal, a simple monosynaptic reflex effected via synapses between sensory neurons innervating the siphon and motor neurons innervating the gill. Following long-term habituation training, a profound depression in the efficacy of synaptic transmission (long-term depression; LTD) lasting for more than three weeks was demonstrated (Castellucci et al., 1978). Conversely, a single sensitizing stimulus rapidly restored both the reflex and the efficacy of synaptic transmission to control levels in previously habituated animals (Carew et al., 1979), and long-term sensitization training alone resulted in an increase in efficacy of synaptic transmission (long-term potentiation; LTP) above control levels (Castellucci et al., 1986). These long-term alterations in efficacy of synaptic transmission were subsequently shown to be associated with morphological changes. The number, size, and vesicle complement of sensory neuron presynaptic active zones were increased in long-term sensitized animals and decreased in long-term habituated animals when compared with controls (Bailey and Chen, 1983). The present results indicate that, while the structure of cerebellothalamic dendritic active zones remains fixed, their vesicle complement increases in association with volitional motor adaptation. Thus, similar ultrastructural synaptic changes that accompany behavioral learning in the marine snail have been shown in the present study to accompany behavioral adaptation in the rat. It is also likely that the changes in vesicle complement of sensory neuron presynaptic active zones in the marine snail are at least partly responsible for the LTD and LTP accompanying the behavioral learning. The ultrastructural changes described in the present study, therefore, are also likely to be expressed physiologically as a potentiation of transmission across cerebellothalamic synapses.

Bailey and Chen (1988) also showed an increase in the total number of synaptic varicosities per sensory neuron in *Aplysia* following long-term sensitization training and, conversely, a decrease in varicosities following long-term habituation training. We did not quantitate the number or density of cerebellothalamic synaptic profiles in the shoulder adduction area of thalamus in the present study. However, an increase on the experimental side of the brain is suggested when we look along the numbers of profiles analyzed in each animal (see Fig. 4A). There are generally greater numbers on the experimental side in almost every experimental animal, whereas no such trend appears in the control and placebo animals (remember that data collection and analysis were performed blind, and the same amount of thalamic tissue was analyzed from each side of the brain in each animal). Thus, in addition to the increase in docked vesicles within cerebellothalamic synapses, there could be an increase in the number of synapses occurring in association with the behavioral adaptation. Further quantitative studies will be required to verify this idea.

In the mammalian central nervous system, the relationship between synaptic plasticity and synapse morphology has been studied mostly in the hippocampus. Synaptic ultrastructure at this site was examined during both the induction (1 hour after high-frequency stimulation) and maintenance (13 days after high-frequency stimulation) phases of LTP in rat (Geinisman, 1993; Geinisman et al., 1991, 1993, 1996). This laboratory reported an increase in the number of perforated axospinous synapses during LTP induction and both a return in the number of perforated axospinous synapses to control levels and an increase in the number of perforated axodendritic synapses during LTP maintenance. No measures of synaptic vesicle docking were performed. These findings led to the proposal that different phases of hippocampal LTP are associated with synapse restructuring whereby axospinous synapses change into axodendritic synapses and vice versa. Buchs and Muller (1996) reported a threefold increase in the number of hippocampal synaptic profiles with perforated active zones, larger apposition zones between pre- and postsynaptic structures, longer postsynaptic densities, and enlarged spine profiles 30–40 minutes following LTP induction. Because cerebellothalamic synapses form active zones simultaneously with dendrites and spines, similar types of structural changes may occur in association with different phases of the learning process. Experiments are currently underway to examine cerebellothalamic synapse ultrastructure at day 7 of behavioral training. It is at this time point that the animals were about mid-way through the rising phase of the motor adaptation (Fig. 1D), and a comparison of ultrastructure at days 7 and 21 may reveal an association between synaptic morphology and different phases of adaptation.

What are the implications of the present findings in terms of cerebellar function? The increase in proportion of active zone occupied by docked vesicles most likely translates to an increase in neurotransmitter release, leading to a potentiation of transmission across the cerebellothalamic synapse. Indeed, preliminary data from rat brain slice experiments in our laboratory indicates that intracellularly recorded excitatory postsynaptic potentials can be potentiated for up to 2 hours following high-frequency electrical stimulation of cut cerebellothalamic afferents. However, we in no way wish to assert that this is the site of synaptic plasticity underlying the cerebellums proposed role in motor learning. LTD and LTP have now been demonstrated at a number of sites along the input and output pathways of the cerebellum (Ito et al., 1982; Ito and Kano, 1982; Rawson and Tilokskulchai, 1982; Ekerot and Kano, 1985; Racine et al., 1986; Sakurai, 1987; Iriki et al., 1989, 1991; Meftah and Rispal-Padel, 1994; Pananceau et al., 1996), and it is likely that each of these sites plays a specific role in the learning process. Interestingly, recent studies of the cellular basis of learning in *Aplysia californica* indicate that the associated synaptic plasticity is far more complex and occurs at many more sites than originally proposed for this system also (Glanzman, 1995). To our knowledge, there is only one other laboratory that has addressed the question of synaptic plasticity at the cerebel-

Fig. 5. Data pertaining to the axodendritic active zone. Format is the same as that explained in Figure 4. **A:** Summed length of all subzones and gaps per synaptic profile. **B:** Summed length of all subzones per synaptic profile. **C:** Summed length of all gaps per synaptic profile. **D:** Number of shaft subzones per synaptic profile. **E:** Proportion of subzones with docked synaptic vesicles per synaptic profile. The significant differences in summed length of all subzones in rat 9 and the number of subzones in rats 9 and 10 are likely to be associated with the same sampling bias that led to the significant differences observed in Figure 4A (rats 9 and 10) rather than with motor adaptation (see Results section). The significant increase on the experimental side in the proportion of subzones with docked synaptic vesicles is the only ultrastructural change of all those quantitated that is likely to be associated with the motor adaptation.

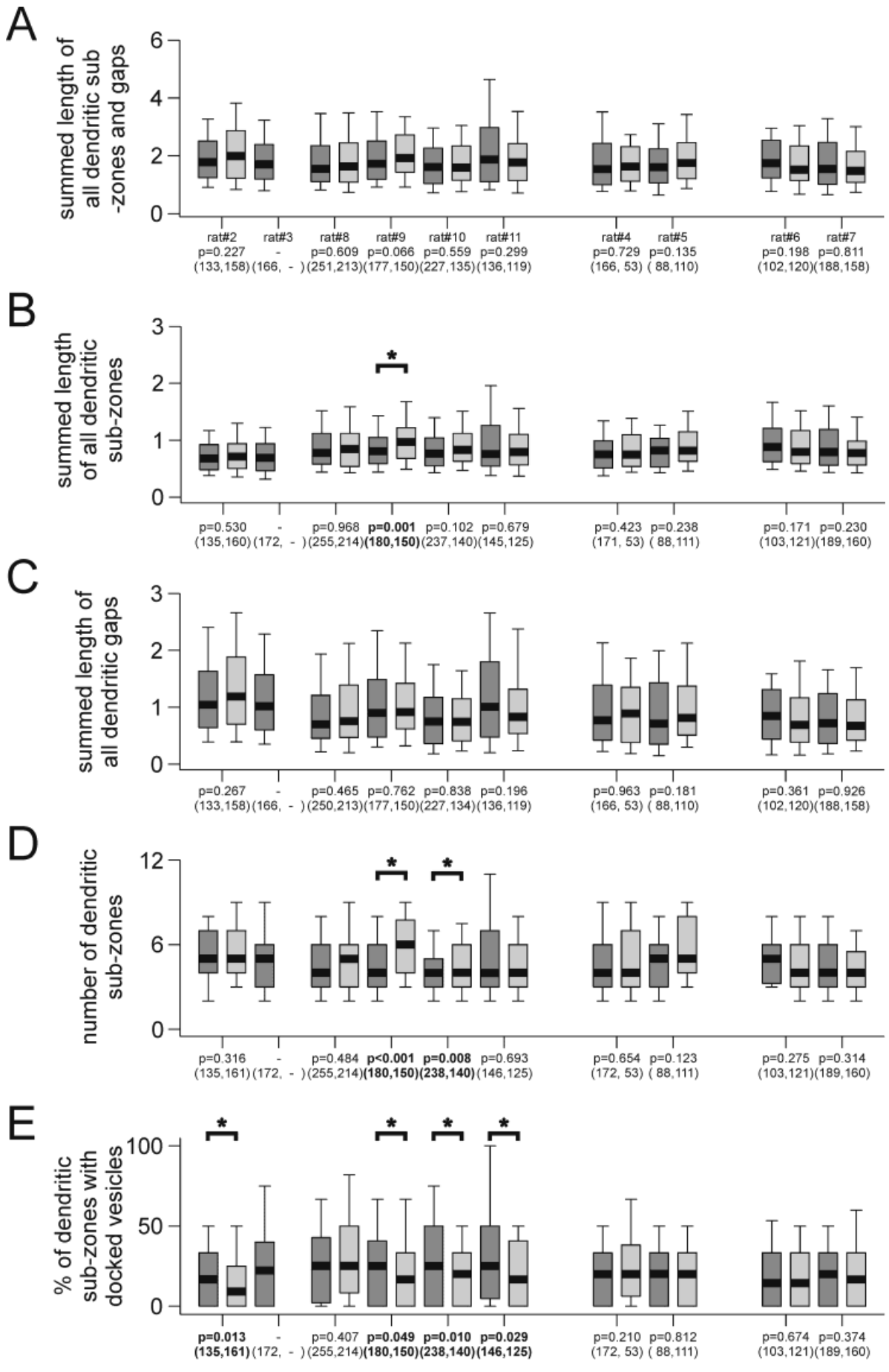
A
summed length of all dendritic sub -zones and gaps
6
4
2
0
rat#2 rat#3 rat#8 rat#9 rat#10 rat#11 rat#4 rat#5 rat#6 rat#7
p=0.227 - p=0.609 p=0.066 p=0.559 p=0.299 p=0.729 p=0.135 p=0.198 p=0.811
(133,158) (166, -) (251,213) (177,150) (227,135) (136,119) (166, 53) (88,110) (102,120) (188,158)
B
summed length of all dendritic sub-zones
3
2
1
0
*
p=0.530 - p=0.968 p=0.001 p=0.102 p=0.679 p=0.423 p=0.238 p=0.171 p=0.230
(135,160) (172, -) (255,214) (180,150) (237,140) (145,125) (171, 53) (88,111) (103,121) (189,160)
C
summed length of all dendritic gaps
3
2
1
0
p=0.267 - p=0.465 p=0.762 p=0.838 p=0.196 p=0.963 p=0.181 p=0.361 p=0.926
(133,158) (166, -) (250,213) (177,150) (227,134) (136,119) (166, 53) (88,110) (102,120) (188,158)
D
number of dendritic sub-zones
12
6
0
* *
p=0.316 - p=0.484 p<0.001 p=0.008 p=0.693 p=0.654 p=0.123 p=0.275 p=0.314
(135,161) (172, -) (255,214) (180,150) (238,140) (146,125) (172, 53) (88,111) (103,121) (189,160)
E
% of dendritic sub-zones with docked vesicles
100
50
0
* * * *
p=0.013 - p=0.407 p=0.049 p=0.010 p=0.029 p=0.210 p=0.812 p=0.674 p=0.374
(135,161) (172, -) (255,214) (180,150) (238,140) (146,125) (172, 53) (88,111) (103,121) (189,160)

Figure 5

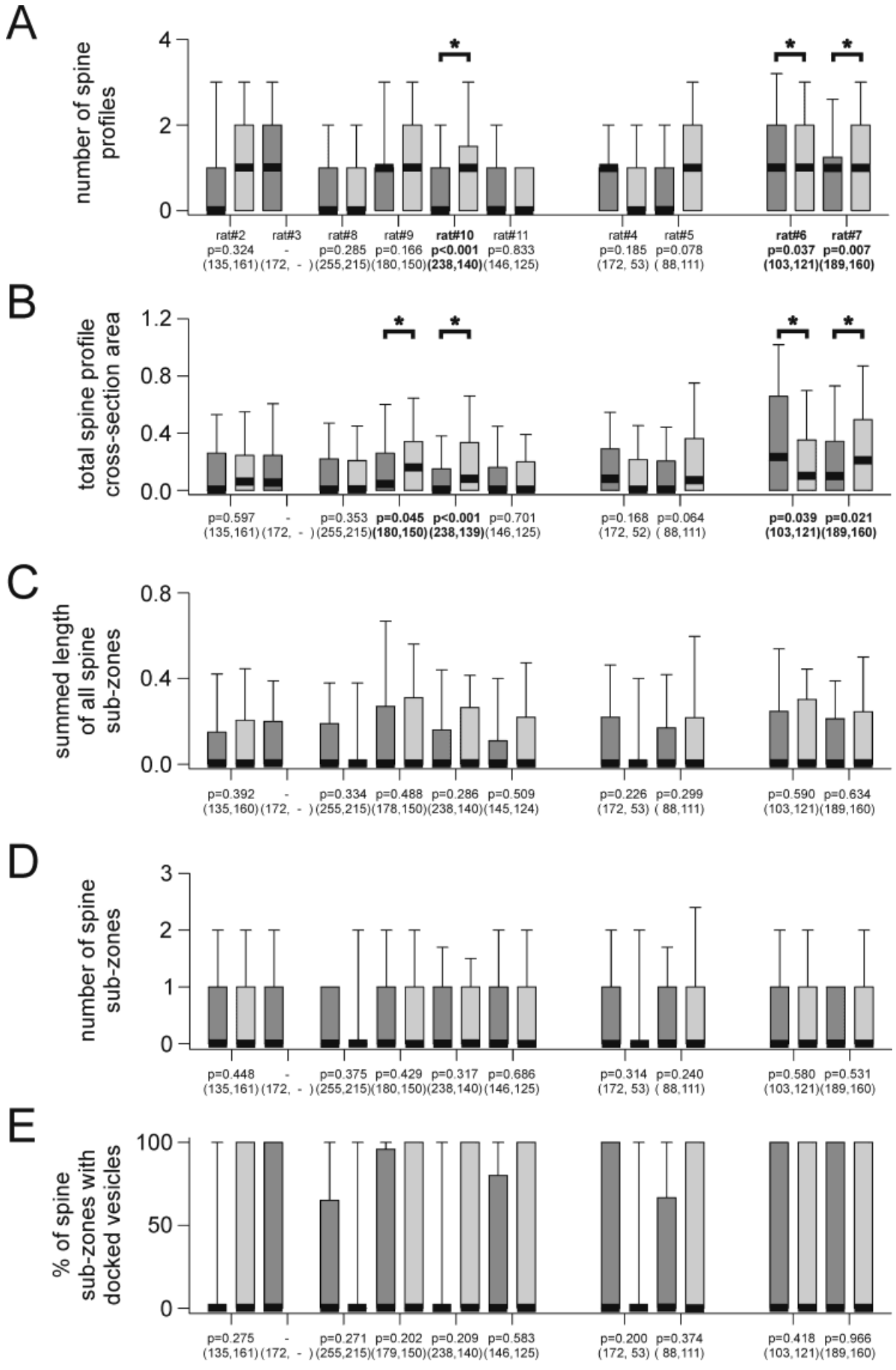
A
number of spine profiles
4
2
0
*
*
*
rat#2 rat#3 rat#8 rat#9 rat#10 rat#11 rat#4 rat#5 rat#6 rat#7
p=0.324 - p=0.285 p=0.166 p<0.001 p=0.833 p=0.185 p=0.078 p=0.037 p=0.007
(135,161) (172, -) (255,215) (180,150) (238,140) (146,125) (172, 53) (88,111) (103,121) (189,160)
B
total spine profile cross-section area
1.2
0.8
0.4
0.0
*
*
*
*
p=0.597 - p=0.353 p=0.045 p<0.001 p=0.701 p=0.168 p=0.064 p=0.039 p=0.021
(135,161) (172, -) (255,215) (180,150) (238,139) (146,125) (172, 52) (88,111) (103,121) (189,160)
C
summed length of all spine sub-zones
0.8
0.4
0.0
p=0.392 - p=0.334 p=0.488 p=0.286 p=0.509 p=0.226 p=0.299 p=0.590 p=0.634
(135,160) (172, -) (255,215) (178,150) (238,140) (145,124) (172, 53) (88,111) (103,121) (189,160)
D
number of spine sub-zones
3
2
1
0
p=0.448 - p=0.375 p=0.429 p=0.317 p=0.686 p=0.314 p=0.240 p=0.580 p=0.531
(135,161) (172, -) (255,215) (180,150) (238,140) (146,125) (172, 53) (88,111) (103,121) (189,160)
E
% of spine sub-zones with docked vesicles
100
50
0
p=0.275 - p=0.271 p=0.202 p=0.209 p=0.583 p=0.200 p=0.374 p=0.418 p=0.966
(135,161) (172, -) (255,215) (179,150) (238,140) (146,125) (172, 53) (88,111) (103,121) (189,160)

Figure 6

lothalamic relay. Using a novel type of classical conditioning paradigm in cats, Rispal-Padel and Meftah (1992) demonstrated a long-lasting increase in forelimb flexion amplitude evoked by electrical stimulation of the cerebellothalamocortical pathway. They also provided some evidence that thalamocortical rather than cerebellothalamic synapses were largely responsible for the supposed plastic changes in the capacity of the cerebellar efferent pathways to produce enhanced effects on the musculature (Rispal-Padel and Meftah, 1992; Meftah and Rispal-Padel, 1994). It remains to be determined whether the apparent differences in the findings of the two laboratories can be explained by differences in the types of learning paradigms employed (our paradigm can best be described as nonassociative learning, whereas theirs is clearly associative), or the fact that we have not yet examined the degree of structural plasticity that may or may not be induced at thalamocortical synapses by our behavioral paradigm. In relation to the first possibility, a number of differences in nonassociative and associative cellular mechanisms of learning have been described for invertebrates and vertebrates (for review, see Hawkins et al., 1993), and it is therefore possible that synaptic plasticity occurs at different locations along a given pathway depending on the type of behavior to be learned. On the other hand, if it transpires that our paradigm induces far greater plasticity at thalamocortical synapses than at cerebellothalamic synapses, then our findings could be consistent with those using the classical conditioning paradigm.

Finally, we would like to emphasize some of the advantages the motor system has over the cognitive system as a model of learning and memory. The establishment of a causal relationship between long-term changes in the efficacy of synaptic transmission and learning and memory in the mammalian brain has been hampered in the hippocampus, where LTP was first described, by the lack of any clearly defined functional or behavioral localization in this structure (i.e., it is difficult to correlate anatomical or physiological change with a particular learning paradigm). The present model of volitional motor adaptation overcomes this problem in a number of ways. The first is the relative ease by which the learned behavior can be monitored and described. Second, the learned behavior can be restricted to one limb, thus providing the contralateral limb as an internal control. Third, because the neural circuitry responsible for the control or execution of movement is organized along topographical lines throughout the motor system, we can use combined physiological and anatomical techniques to identify the tissue to be studied with a reasonable degree of confidence that any effect which behavioral adaptation might have on the tissue will remain detectable following analysis.

Fig. 6. Data pertaining to the axospinous contacts. Format is the same as that explained in Figure 4. **A:** Number of spine profiles per synaptic profile. **B:** Total spine profile cross-sectional area per synaptic profile. **C:** Summed length of all spine subzones per synaptic profile. **D:** Number of spine subzones per synaptic profile. **E:** Proportion of spine subzones with docked vesicles per synaptic profile. The significant differences in the number of spine profiles in rat 10 and total spine profile cross-sectional area in rats 9 and 10 are likely to be associated with the same sampling bias that led to the significant differences observed in Figure 4A (rats 9 and 10) rather than with motor adaptation (see Results section). Synaptic profiles without spine profiles have been included in these data, which is the reason the median values are heavily weighted toward zero in A–E. Also, spine profiles without active zones have been included, which is the reason the median values are even more heavily weighted toward zero in C–E. Therefore, the data presented in this figure are somewhat misleading (e.g., almost every spine subzone observed in these experiments had docked synaptic vesicles). However, we analyzed subsets of these data with synaptic profiles without spine profiles and spine profiles without active zones removed where appropriate, and the results were almost identical as they appear here.

ACKNOWLEDGMENTS

We gratefully acknowledge the technical assistance of Anthony Natoli, Doris Tomas, and Sue Connell.

LITERATURE CITED

Albus JS. 1971. A theory of cerebellar function. Math Biosci 10:25–61.

Aumann TD, Horne MK. 1996. A comparison of the ultrastructure of synapses in the cerebello-rubral and cerebello-thalamic pathways in the rat. Neurosci Lett 211:175–178.

Aumann TD, Rawson JA, Finkelstein DI, Horne MK. 1994. Projections from the lateral and interposed cerebellar nuclei to the thalamus of the rat: a light and electron microscopic study using single and double anterograde labelling. J Comp Neurol 349:165–181.

Bailey CH, Chen M. 1983. Morphological basis of long-term habituation and sensitization in *Aplysia*. Science 220:91–93.

Bailey CH, Chen M. 1988. Long-term memory in *Aplysia* modulates the total number of varicosities of single identified sensory neurons. Proc Natl Acad Sci USA 85:2373–2377.

Buchs PA, Muller D. 1996. Induction of long-term potentiation is associated with major ultrastructural changes at activated synapses. Proc Natl Acad Sci USA 93:8040–8045.

Carew TJ, Castellucci VF, Kandel ER. 1979. Sensitization in *Aplysia*: restoration of transmission in synapses inactivated by long-term habituation. Science 205:417–419.

Carlin RK, Siekevitz P. 1983. Plasticity in the central nervous system: do synapses divide? Proc Natl Acad Sci USA 80:3517–3521.

Castellucci VF, Carew TJ, Kandel ER. 1978. Cellular analysis of long-term habituation of the gill-withdrawal reflex of *Aplysia californica*. Science 202:1306–1308.

Castellucci VF, Frost WN, Goelet P, Montarolo PG, Schacher S, Morgan JA, Blumenfeld H, Kandel ER. 1986. Cell and molecular analysis of long-term sensitization in *Aplysia*. J Physiol (Paris) 81:349–357.

Dyson SE, Jones DG. 1984. Synaptic remodeling during development and maturation: junction differentiation and splitting as a mechanism for modifying connectivity. Brain Res 315:125–137.

Ekerot CF, Kano M. 1985. Long-term depression of parallel fiber synapses following stimulation of climbing fibers. Brain Res 341:357–360.

Geinisman Y. 1993. Perforated axospinous synapses with multiple, completely partitioned transmission zones: probable structural intermediates in synaptic plasticity. Hippocampus 3:417–434.

Geinisman Y, Morrell F, De Toledo-Morrell L. 1989. Perforated synapses on doubleheaded dendritic spines: a possible structural substrate of synaptic plasticity. Brain Res 480:326–329.

Geinisman Y, De Toledo-Morrell L, Morrell F. 1991. Induction of long-term potentiation is associated with an increase in the number of axospinous synapses with segmented post-synaptic densities. Brain Res 566:77–88.

Geinisman Y, De Toledo-Morrell L, Morrell F, Heller RE, Rossi M, Parshall RF. 1993. Structural synaptic correlate of long-term potentiation: formation of axospinous synapses with multiple, completely partitioned transmission zones. Hippocampus 3:435–446.

Geinisman Y, De Toledo-Morrell L, Morrell F, Persina IS, Beatty MA. 1996. Synapse restructuring associated with the maintenance phase of hippocampal long-term potentiation. J Comp Neurol 368:413–423.

Glanzman DL. 1995. The cellular basis of classical conditioning in *Aplysia californica*—it's less simple than you think. TINS 18:30–36.

Greenough WT, West RW, De Voogd TJ. 1978. Subsynaptic plate perforations: changes with age and experience in the rat. Science 202:1096–1098.

Grofova I, Rinvik E. 1974. Cortical and pallidal projections to the nucleus ventralis lateralis thalami. Electron microscopical studies in the cat. Anat Embryol (Berl) 146:113–132.

Hallanger AE, Levey AI, Lee HJ, Rye DB, Wainer BH. 1987. The origins of cholinergic and other subcortical afferents to the thalamus in the rat. J Comp Neurol 262:105–124.

Hallanger AE, Price SD, Lee HJ, Steininger TL, Wainer BH. 1990. Ultrastructure of cholinergic synaptic terminals in the thalamic anteroventral, ventroposterior, and dorsal lateral geniculate nuclei of the rat. J Comp Neurol 299:482–492.

Harding BN. 1973a. An ultrastructural study of the centre median and ventrolateral thalamic nuclei of the monkey. Brain Res 54:335–340.

Harding BN. 1973b. An ultrastructural study of the termination of afferent fibers within the ventrolateral and centre median nuclei of the monkey thalamus. Brain Res 54:341–346.

Harding BN, Powell TPS. 1977. An electron microscopic study of the centre median and ventrolateral nuclei of the thalamus in the monkey. Phil Trans R Soc Lond (Biol) 279:359–412.

Hawkins RD, Kandel ER, Siegelbaum SA. 1993. Learning to modulate transmitter release: themes and variations in synaptic plasticity. Annu Rev Neurosci 16:625–665.

Hebb DO. 1949. The organization of behavior. New York: John Wiley & Sons.

Holmes G. 1917. The symptoms of acute cerebellar injuries due to gunshot injuries. Brain 40:461–535.

Ilinsky IA. 1990. Structural and connectional diversity of the primate motor thalamus: experimental light and electron microscopic studies in the Rhesus monkey. Stereotact Funct Neurosurg 54:114–124.

Iriki A, Pavlides C, Keller A, Asanuma H. 1989. Long-term potentiation in the motor cortex. Science 245:1385–1387.

Iriki A, Pavlides C, Keller A, Asanuma H. 1991. Long-term potentiation of thalamic input to the motor cortex induced by coactivation of thalamocortical and corticocortical afferents. J Neurophysiol 65:1435–1441.

Ito M, Kano M. 1982. Long-lasting depression of parallel fibre–Purkinje cell transmission induced by conjunctive stimulation of parallel fibers and climbing fibers in the cerebellar cortex. Neurosci Lett 33:253–258.

Ito M, Sakurai M, Tongroach P. 1982. Climbing fibre–induced depression of both mossy fibre responsiveness and glutamate sensitivity of cerebellar Purkinje cells. J Physiol (Lond) 324:113–145.

Jones BE, Moore RY. 1977. Ascending projections of the locus coeruleus in the rat. II. Autoradiographic study. Brain Res 127:23–53.

Jones DG, Itarat W, Calverley RKS. 1991. Perforated synapses and plasticity: a developmental overview. Mol Neurobiol 5:217–228.

Jones EG. 1985. The thalamus. New York: Plenum Press.

Konorski J. 1948. Conditioned reflexes and neuron organisation. Cambridge: Cambridge University Press.

Kultas-Ilinsky K, Ilinsky IA. 1991. Fine structure of the ventral lateral nucleus (VL) of the *Macaca mulatta* thalamus: cell types and synaptology. J Comp Neurol 314:319–349.

Kultas-Ilinsky K, Taylor J, Smith KR. 1976. Electron microscopy of corticothalamic degeneration in the rat. Anat Rec 184:454.

Levey AI, Hallanger AE, Wainer BH. 1987. Choline acetyltransferase immunoreactivity in the rat thalamus. J Comp Neurol 257:317–332.

Lindvall O, Björklund A, Nobin A, Stenevi U. 1974. The adrenergic innervation of the rat thalamus as revealed by the glyoxylic acid fluorescence method. J Comp Neurol 154:317–348.

Lund RD, Webster KE. 1967a. Thalamic afferents from the dorsal column nuclei: an experimental anatomical study in the rat. J Comp Neurol 130:301–312.

Lund RD, Webster KE. 1967b. Thalamic afferents from the spinal cord and trigeminal nuclei: an experimental anatomical study in the rat. J Comp Neurol 130:313–328.

Marr D. 1969. A theory of cerebellar cortex. J Physiol (Lond) 202:437–470.

Meftah EM, Rispal-Padel L. 1994. Synaptic plasticity in the thalamocortical pathway as one of the neurobiological correlates of forelimb flexion conditioning: electrophysiological investigation in the cat. J Neurophysiol 72:2631–2647.

Nothias F, Onteniente B, Roudier F, Peschanski M. 1988. Immunocytochemical study of serotoninergic and noradrenergic innervation of the ventrobasal complex of the rat thalamus. Neurosci Lett 95:59–63.

Pananceau M, Rispal-Padel L, Meftah EM. 1996. Synaptic plasticity of the interpositorubral pathway functionally related to forelimb flexion movements. J Neurophysiol 75:2542–2561.

Paxinos G, Watson C. 1998. The Rat Brain in Stereotaxic Coordinates (4th edition). San Diego: Academic Press.

Peschanski M, Besson JM. 1984. Diencephalic connections of the raphae nuclei of the rat brainstem: an anatomical study with reference to the somatosensory system. J Comp Neurol 224:509–534.

Pierce JP, Lewin GR. 1994. An ultrastructural size principle. Neuroscience 58:441–446.

Racine RJ, Wilson DA, Gingell R, Sunderland D. 1986. Long-term potentiation in the interpositus and vestibular nuclei in the rat. Exp Brain Res 63:158–162.

Rawson JA, Tilokskulchai K. 1982. Climbing fibre modification of cerebellar Purkinje cell responses to parallel fibre inputs. Brain Res 237:492–497.

Raymond JL, Lisberger S, Mauk MD. 1996. The cerebellum: a neuronal learning machine? Science 272:1126–1131.

Reynolds ES. 1963. The use of lead citrate at high pH as an electron-opaque stain in electron microscopy. J Cell Biol 17:208–212.

Rinvik E, Grofova I. 1974a. Light and electron microscopical studies of the normal nuclei ventralis lateralis and ventralis anterior thalami in the cat. Anat Embryol (Berl) 146:57–93.

Rinvik E, Grofova I. 1974b. Cerebellar projections to the nuclei ventralis lateralis and ventralis anterior thalami. Anat Embryol (Berl) 146:95–111.

Rispal-Padel L, Meftah EM. 1992. Changes in motor responses induced by cerebellar stimulation during classical forelimb flexion conditioning in cat. J Neurophysiol 68:908–926.

Sakurai M. 1987. Synaptic modification of parallel fibre–Purkinje cell transmission in in vitro guinea pig cerebellar slices. J Physiol (Lond) 394:463–480.

Sawyer SF, Martone ME, Groves PM. 1991. A GABA immunocytochemical study of rat motor thalamus: light and electron microscopic observations. Neuroscience 42:103–124.

Sawyer SF, Tepper JM, Groves PM. 1994. Cerebellar responsive neurons in the thalamic ventroanterior–ventrolateral complex of rats: light and electron microscopy. Neuroscience 63:725–745.

Swanson LW, Hartman BK. 1975. The central adrenergic system. An immunofluorescence study of the location of cell bodies and their efferent connections in the rat utilizing dopamine-beta-hydroxylase as a marker. J Comp Neurol 163:467–505.

Williams MN, Faull RL. 1987. The distribution and morphology of identified thalamo-cortical projection neurons and glial cells with reference to the question of interneurones in the ventrolateral nucleus of the rat thalamus. Neuroscience 21:767–780.